# Electrochemical dissolution of $U_{1-y}Gd_yO_{2\pm x}$:
# Effect of Gd doping on various oxidation state of $UO_{2\pm x}$ matrix

Jandee Kim[a], Jeongmook Lee[a], Young-Sang Youn[a], Nazhen Liu[b], Jong-Goo Kim[a], Yeong-Keong Ha[a], Sang-Eun Bae[a], David W. Shoesmith and Jong-Yun Kim[a,*]

*[a]Nuclear Chemistry Research Division, KAERI, Daejeon, 34057, Korea*
*[b]Department of Chemistry, Western University, London, Ontario N6A 5B7, Canada*
*kimjd@kaeri.re.kr*

## 1. Introduction

SNF (Spent nuclear fuel) is consisted with mainly $UO_2$, radioactive fission products and actinides species. Because the major radio nuclides are located within the oxide matrix, their release rates to the groundwater will be depended on the fuel corrosion/dissolution rate [1-2]. The key factors to determine the $UO_2$ dissolution behaviors, can control the reactivity of the $UO_2$ matrix, are (i) stoichiometry of $UO_{2\pm x}$ matrix; (ii) rare earth (RE) element doping in $UO_2$ matrix; and (iii) environmental condition including chemical composition and pH of water to contact with [3-5].

Because oxide matrix in spent nuclear fuel is consisted with stoichiometric $UO_2$, and also parts of hypo-, and hyper-stoichiometric $UO_{2\pm x}$ matrix, it is important to comprehend chemical and physical properties of matrix depend on differential stoichiometry from dissolution behavior, which determine the release of radionuclides [3-4]. Shoesmith group reported that different local corrosion kinetics of stoichiometric and non-stoichiometric $UO_{2+x}$, determined by SECM approach curves in the presence of oxidant at the corrosion potential [4].

Also, the oxidation of $UO_2$ doped with RE (Rare earth) element has been investigated expensively for decades, in order to determine the effect of fission-product impurities present in solid solution in used fuel [9-11]. RE doped $UO_2$ shows enhanced stability of the cubic fluorite structures of $U_4O_9$-type with respect to $U_3O_8$-type depending on the sintering atmosphere as compared to un-doped $UO_2$ [5-6]. Ho and Radford reported that charge compensation in the Gd-doped urania can be described with formation of oxygen vacancy, oxidation of $U^{4+}$ to $U^{6+}$ via $U^{5+}$, interstitial formation or combination of defect types [7].

Although such substantial efforts have been done, integrated research of stoichiometry and Gd-doping effects have received little interest. And also, there are difficulties to handle the nuclear fuel carefully not to spoil the intrinsic properties of itself. Especially, in determining dissolution behaviors of fuel, electrochemical techniques are very powerful and reliable tool to establish the thermodynamic values presented dissolution kinetics. Another important change expected to influence the reactivity of the fuel is the rare earth doping which will change the conductivity and structural properties of the $UO_2$ matrix.

In this work, non-stoichiometric (hypo-, hyper-stoichiometric $UO_{2\pm x}$) and stoichiometric $UO_2$, and/or low and highly doped $U_{1-y}Gd_yO_{2\pm x}$ were manufactured by mechanical blending method followed by oxidation with control the oxygen potential. Stoichiometry of all pellets was determined and distinguished into hypo-, hyper-, and stoichiometric $UO_{2\pm x}$ by analysis with using non-destructive X-ray method, conveniently. And influences of non-stoichiometric urania matrix and Gd dopant on dissolution behaviors of $UO_{2\pm x}$ matrix were investigated by electrochemical study.

## 2. Methods and Results

### 2.1 Preparation of $U_{1-y}Gd_yO_{2\pm x}$ pellets

The un-irradiated $UO_2$ and Gd doped $UO_2$ pellets are fabricated by sintering pressed green pellets at ~1700 ℃ in a reducing atmosphere, which are prepared by blending method to grain $UO_2$ powders and/or $Gd_2O_3$ containing $UO_2$ powders followed pressing with 300 MPa. The doped Gd amounts were 1 and 10 mol% contrasting with uranium, respectively. All green pellets were weighed before and after sintering process to estimate additional or missing oxygen. Pellets were sintered on alumina crucible in a linear type of furnace at 1700℃ in a reducing atmosphere of Ar-4 % of $H_2$ for 24 hrs. Because hypo-stoichiometric $UO_{2-x}$ was manufactured by this reducing condition, hyper-, and stoichiometric ones were adjusted by followed mild oxidation step control the oxygen potential by regulation of $CO/CO_2$ mixed gas ratio from 10 to 0.001, temperatures (800-1500°C) and Gd contents (mol%), according to the Ellingham diagram. Prepared pellets have ~8 mm dia. and less than 1 mm thickness.

### 2.2 Grain structure and growth rates

Scanning electron microscopic results, using 20 keV electron acceleration voltage with 10 mm of working distance, revealed morphological evolutions and grain features of freshly prepared pellet depending on Gd-doped level and stoichiometry.

The grain structures of $U_{1-y}Gd_yO_{2\pm x}$ changed drastically depend on Gd-doped level as shown in Fig. 1.
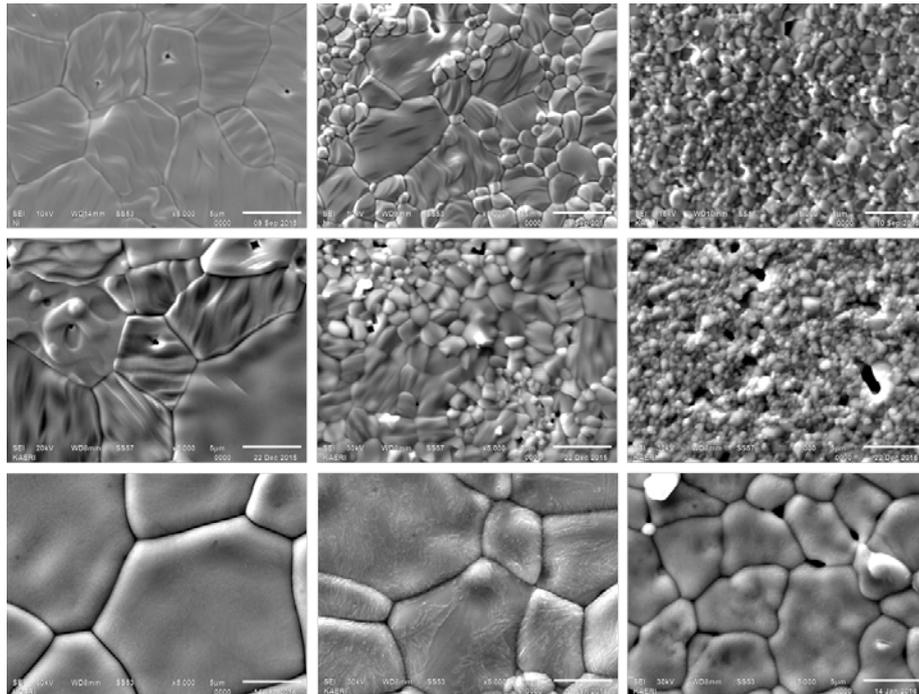
Fig. 1 structural changes of grains on as prepared (a-c) hypo-stoichiometric; (d-f) stoichiometric and (g-i) hyper-stoichiometric $U_{1-y}Gd_yO_{2\pm x}$ depend on Gd contents which are (a,d,g) 0; (b,e,h) 1; and (c,f,i) 10 mol%. Magnifications of SEM images are ×3000, and scale bar presents 5 μm length.

In case of un-doped hypo-stoichiometric $UO_{2-x}$ (Fig. 1(a)), it has polygonal structures consisted of wrinkled and flattened domains, are observed ~5 to ~10 μm sized, and the domain size decreases rapidly with increase of Gd doping level (Fig. 1(b-c)).

On the other hand, stoichiometric and hyper-stoichiometric pellets prepared by through the $CO/CO_2$ oxidation of hypo-stoichiometric pellets, have more big domains of over 20 um sized and smooth textured surface as shown in Fig. 1(d-i). The interstitial oxygen activates internal strain of distorted cubic lattice, followed by enhanced uranium diffusion results in crystalline growths. Therefore, it can be explained that the distribution of excess $O^{2-}$ makes to develop domain growth affects to domain structures of various size, texture and figurations. And as Gd-doping level increase, grain features got small in non-stoichiometric and stoichiometric pellets. However, hyper-stoichiometric pellets showed tolerance toward size-change to small. Probably, Gd plays a role to prevent inflowing of extrinsic oxygen into hyper-$UO_{2+x}$ matrix. In fact, oxidation process of un-doped $UO_{2-x}$ to $UO_{2+x}$ needed more high oxygen potential than 10 mol% Gd-doped $UO_{2-x}$.

## 2.3 Electrochemical behaviors

Fig. 2 shows CV recorded in carbonate solution with rotating electrode in scanning potential range from -3 V to 4 V, which can show catalytic behavior of water decomposition according to Gd-doping.
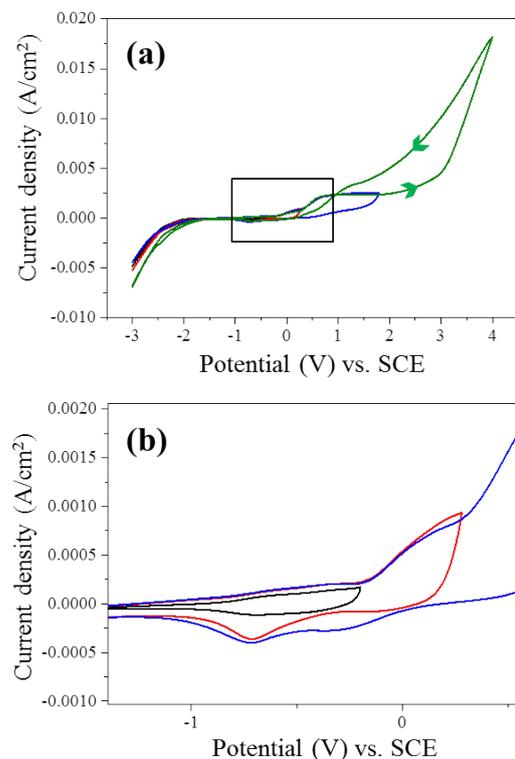


Fig. 2 (a) CV of hypo-stoichiometric $UO_{2-x}$ with varying potential window demonstrates two distinguishable oxidation mechanism. (b) the magnified inset of (a) indicated with rectangle. Electrolyte is 0.1 M $[HCO_3^-/CO_3^{2-}]$ solution in 0.1 M $NaClO_4$ at pH=8.9. Scan rate is 0.05 Vsec$^{-1}$, and electrode was rotated with 2000 rpm.

In forward scanning, two kinds of distinguishable anodic oxidation currents were appeared at ~ 0 V (red CV) and above 0.2 V (blue one). Prior oxidation peak indicates forming a thin surface oxide layer mixed with U(IV) and U(V). Further oxidation brings more large anodic currents for the oxidative dissolution of oxide matrix to soluble uranyl ($UO_2^{2+}$) species by forming $UO_2CO_3$, observed at above 0.2 V. And reduction currents according to reduction of dissolved $UO_2^{2+}$ occur at −0.7 V in reverse scanning of potential.

surface oxidation:
$UO_2 + 0.33H_2O \rightarrow UO_{2.33} + 0.66H^+ + 0.66e$

dissolutive oxidation:
$UO_{2.33} + 0.66H^+ \rightarrow UO_2^{2+} + 0.33H_2O + 1.34e$.

Distinguished two oxidation peaks, indicating two steps of oxidation mechanisms, defined as surface oxidation and dissolutive oxidation, respectively. Because dissolution process includes these whole oxidation mechanisms, oxidative behaviors of each steps has been investigated to understand the dissolution of $U_{1-y}Gd_yO_{2\pm x}$.

Anodic Tafel curves for each oxidation mechanisms were obtained from LSV (Linear sweep voltammetry) separated into two-oxidative components. Tafel slope provides Tafel constant (α), which show the rate of oxidation kinetics as bellowed equation.

Tafel slope ($b_a$)
= $\Delta E / \Delta \log i = 2.3RT/\alpha nF$

The kinetic of surface oxidation (α1), which is the starting point of dissolution process, in Figure 3(a) shows hypo-, and hyper-stoichiometric un-doped pellets are faster than stoichiometric one, however, as Gd doping level increase, the kinetic rates are dramatically decrease to similar value of Tafel constant (stoichiometric pellets are engaged in doing experiment.). On the other hand, the kinetic rate of dissolutive oxidation (α2 in Fig. 3(b)) presents non-stoichiometric pellets are more stable than stoichiometric one, and hypo- and hyper-stoichiometric $U_{1-y}Gd_yO_{2\pm x}$ have not a big difference though Gd dopant increase. Therefore, Gd doping affects to suppress the surface oxidation, thermodynamically, and also surface oxidation is the primary factor which determines rate of dissolution in $U_{1-y}Gd_yO_{2\pm x}$.

## 3. Conclusion

Stoichiometric and non-stoichiometric Gd-doped $U_{1-y}Gd_yO_{2\pm x}$ pellets are prepared by mechanical blending method adjusting the oxygen potential.
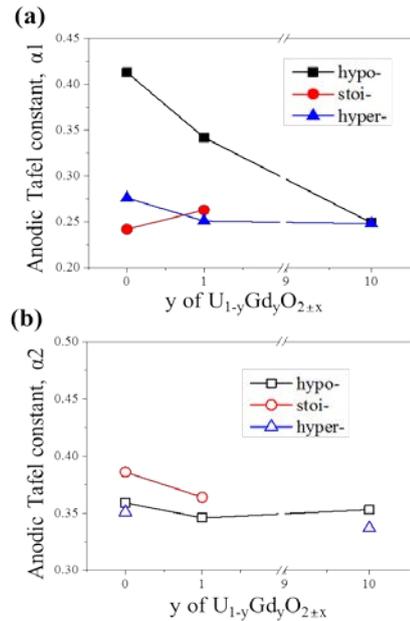


Fig. 3 Anodic Tafel constants of (a) surface oxidation and followed by (b) dissolutive oxidation depend on stoichiometry and Gd-doped amount.

Stoichiometry of all pellets was confirmed by non-destructive X-ray analysis.

The interstitial oxygen in hyper-stoichiometric $U_{1-y}Gd_yO_{2+x}$ improves the uranium diffusion in solid solution to allow grain size to be large.

Oxidative dissolution of $U_{1-y}Gd_yO_{2\pm x}$ can be described with surface oxidation and followed dissolutive oxidation mechanisms. Gd dopants influence on decrease the surface oxidation rate which can control the whole oxidative dissolution reaction.

## References

[1] Rodney C. Ewing, Long-term storage of spent nuclear fuel, Nature Materials, 14 (2015) 252-257.
[2] J. C. Wren, D. W. Shoesmith, S. Sunder, Corrosion behavior of uranium dioxide in alpha radiolytically-decomposed water, J. Electrochem, Soc. (2005) 152.
[3] R.J. McEachern, P. Taylor, J. Nucl. Mater. 254 (1998) 87–121.
[4] H. He, R.K. Zhu, Z. Qin, P. Keech, Z. Ding, D.W. Shoesmith, J. Electrochem. Soc. 156 (2009) C87-C94.
[5] R.J. McEachern, D.C. Doern, D.D. Wood, J. Nucl. Mater. 252 (1998) 145-149.
[6] L.E. Thomas, R.E. Einziger, H.C. Buchanan, J. Nucl. Mater. 201 (1993) 310-319.
[7] S.M. HO, K.C. Radford, Nucl. Technol. 73 (1986) 350-360.